Fracturing, block faulting, and moulin development associated with progressive collapse and retreat of a maritime glacier: Falljökull, SE Iceland

Emrys Phillips,[1] Andrew Finlayson,[1] and Lee Jones[2]

Received 22 March 2013; revised 17 July 2013; accepted 19 July 2013.

[1] Since 2007, Falljökull in southeast Iceland has been undergoing passive downwasting, providing an ideal opportunity to study a range deformation structures developed in response to ice-marginal collapse and retreat. An integrated terrestrial lidar, Ground Penetrating Radar, and glaciological structural study of the clean, debris-free ice at the margin of Falljökull has allowed a detailed model of the surface and subsurface 3D structure to be developed. Collapse of the glacier margin takes the form of a multiple rotational failure controlled by large-scale, down-ice dipping normal faults. As the fault-bound blocks of ice are displaced downslope, they rotate leading to localized compression and the formation of down-faulted graben-like structures. Moulins present within the marginal zone of Falljökull are closely associated with the zones of relatively more intense brittle deformation which crosscut the glacier. A model is proposed where the moulins have formed in response to the progressive collapse of englacial drainage channels located along down-ice dipping normal faults. The preferential development of the moulins and englacial drainage channels along the normal faults weakens the ice along these structures, promoting or even accelerating further collapse of the ice margin. The complex pattern of surface lowering within the marginal zone of Falljökull has also been shown to be directly related to movement on the main faults controlling the collapse of the ice margin. This evidence suggests that structurally controlled collapse may, in some instances, have a profound effect on glacier surface lowering and geodetic mass balance measurements.

Citation: Phillips, E., A. Finlayson, and L. Jones (2013), Fracturing, block faulting, and moulin development associated with progressive collapse and retreat of a maritime glacier: Falljökull, SE Iceland, *J. Geophys. Res. Earth Surf.*, *118*, doi:10.1002/jgrf.20116.

1. Introduction

[2] Published structural glaciological studies have focused upon the structures developed within different glacier types from a wide range of settings, including polythermal [*Hambrey et al.*, 2005], surging [*Sharp*, 1988; *Sharp et al.*, 1988; *Lawson et al.*, 1994; *Lawson*, 1996; *Bennett et al.*, 2000; *Woodward et al.*, 2002], Arctic [*Huddleston and Hooke*, 1980], and alpine glaciers [*Allen et al.*, 1960; *Hambrey and Milnes*, 1977; *Glasser et al.*, 2003; *Goodsell et al.*, 2005; *Herbst et al.*, 2006; *Appleby et al.*, 2010]. These studies have not only contributed to our understanding of the strain histories and structural evolution of these glaciers, but have also shed light on the mechanisms controlling their forward movement and highlighted the importance of deformation structures in controlling sediment distribution within a glacier or its sole. However, structural studies of the deformation occurring within the ice during stagnation and collapse are, in comparison, relatively rare [e.g., *Glasser and Scambos*, 2008].

[3] This study focuses on a range of brittle deformation structures developed within the marginal zone of Falljökull, the southeastern arm of the twin-lobed outlet glacier of Virkisjökull-Falljökull which drains the southern side of Öræfajökull ice cap in southeast Iceland (Figures 1a and 1b). Iceland's glaciers are highly sensitive to climatic fluctuations on an annual to decadal scale. Annual measurements of the position of the front of these glaciers have demonstrated that since 1990 most of Iceland's glaciers have been in retreat, with the rate of retreat having accelerated over the last two decades [*Jóhannesson and Sigurðsson*, 1998; *Sigurðsson et al.*, 2007]. Prior to 2007, Falljökull was undergoing active retreat with forward motion during the winter months leading to the development of a series of recessional moraines [*Bradwell et al.*, 2013]. However, in 2007, there was a major change in the behavior of the glacier, and since this date it has been undergoing passive downwasting and collapse and, therefore, provides an ideal natural laboratory in which to study the range of deformation structures developed in response to ice-marginal retreat. The present multidisciplinary study utilizes terrestrial lidar scanning,

[1]British Geological Survey, Edinburgh, UK.
[2]British Geological Survey, Keyworth, UK.

Corresponding author: E. Phillips, British Geological Survey, Murchison House, West Mains Road, Edinburgh EH9 3LA, UK. (erp@bgs.ac.uk)

©2013. American Geophysical Union. All Rights Reserved.
2169-9003/13/10.1002/jgrf.20116

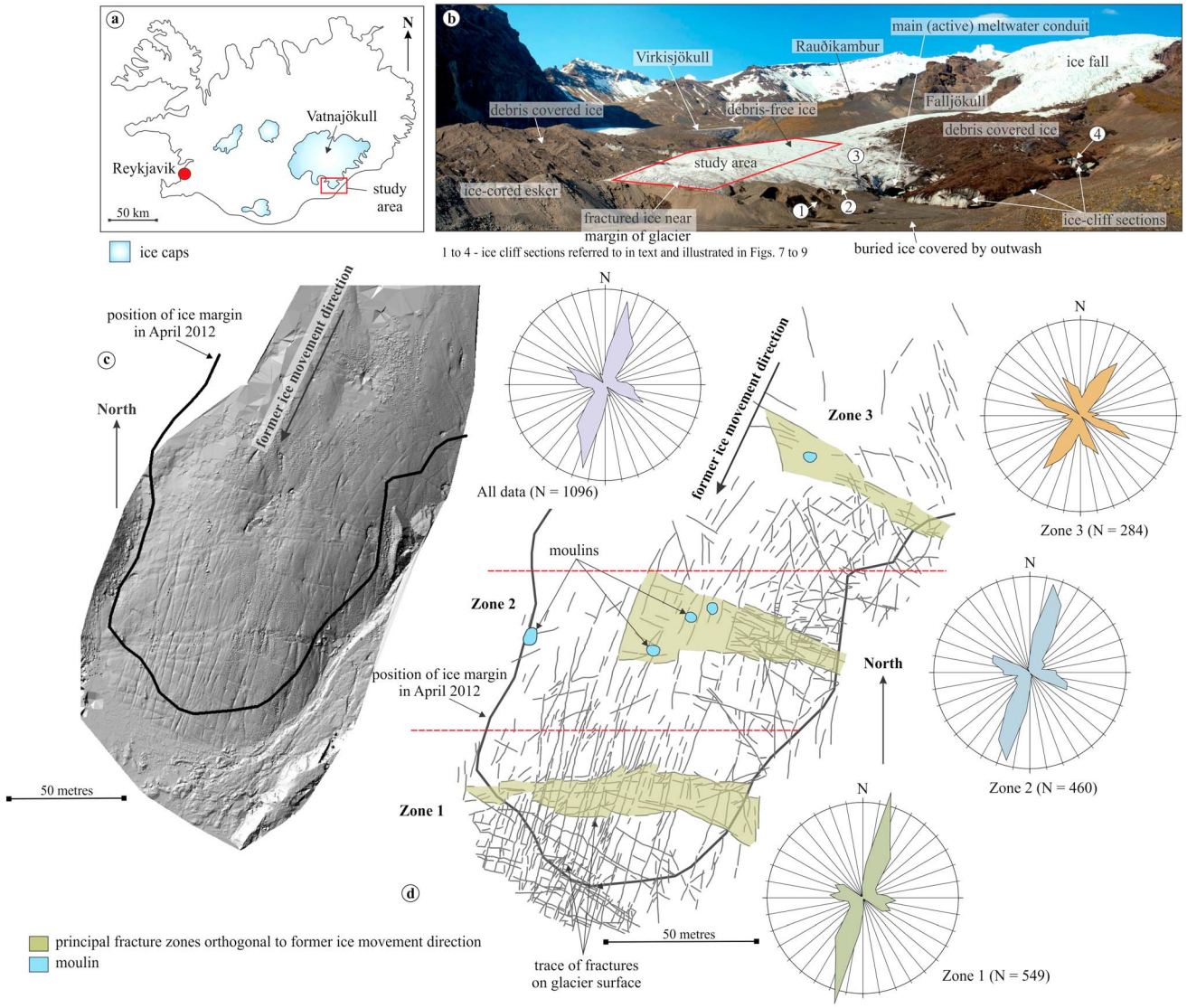

Figure 1. (a) Simplified map of Iceland showing the location of the study area on the southern side of the Vatnajökull ice cap; (b) Photograph of Falljökull and Virkisjökull showing the location of the present study area within the debris-free (clean) ice at the margin of Falljökull (numbers 1 to 4 mark the locations of the ice-cliff locations); (c) Digital Elevation Model (DEM) of the surface of Falljökull derived from the terrestrial lidar scan of the lower part of the glacier; (d) Detailed structural map of the lower part of Falljökull showing the pattern of crosscutting fractures and faults developed within the debris-free clean ice. Also shown are the locations of the moulin developed within this ice-marginal zone. Orientation data (trend) obtained for the fractures are plotted as a series of rose diagrams.

a detailed glaciological structural study, and a Ground Penetrating Radar (GPR) survey to investigate the surface and subsurface 3D structure of the glacier margin. Movement upon large-scale, down-ice dipping brittle faults and the formation of down-faulted graben-like structures are related to ice-block rotation during collapse. A structural control on the location of englacial drainage channels is suggested with both preexisting thrust faults, which accommodated early forward motion of the glacier, and more recently formed normal and reverse faults, associated with its collapse, playing an important role in aiding the passage of meltwater through the glacier.

2. Location of Study Area and Glaciological Setting

[4] The study area occurs close to the terminus of Falljökull, one of a number of outlet glaciers draining the southern side of the Vatnajökull ice cap in southeast Iceland (Figure 1a). This glacier forms the eastern arm of the twin-lobed outlet glacier of Virkisjökull-Falljökull which drains a shared accumulation area located within the western part of the ice-filled summit crater of the stratovolcano Öraefajökull. From their combined source, 2000 m above sea level, the glaciers descend over a steep ice fall. At these higher altitudes (above 600 m), the

two glaciers are separated by a prominent bedrock ridge known as the Rauðikambur (Figure 1b). The glaciers then "merge" down valley where the boundary between them is marked by a wide supraglacial debris band, or medial moraine sourced from this ridge. In the terminal zone of the glaciers, which previously extended 2 to 3 km down valley [*Danish Geodetisk Staff*, 1904; *Guðmundsson*, 1997], this medial moraine forms of a broad area of debris-covered ice (Figure 1b).

[5] In the period since 1932, Virkisjökull-Falljökull has undergone over 1200 m of retreat punctuated by one major advance of approximately 100 m that took place during the 1970s and 1980s [*Guðmundsson*, 1997; *Bradwell et al*., 2013]. Phases of active (dynamic) retreat are marked by two groups of annual push moraines: the older probably formed between 1935 and 1945, based on geomorphological relationships, photographic evidence, and lichenometric data; and the younger between 1990 and 2003, based on field and photographic evidence [*Bradwell et al*., 2013]. *Bradwell et al*. [2013] suggested that during the years of annual push moraine formation the retreating glacier was "dynamic" and undergoing some forward motion in the winter/spring. An increase in the spacing of these moraines in the period between 1998 and 2003 reflects a progressive increase in the loss of mass relative to changes in forward motion of the glacier at its margin, against a backdrop of warming summers. The cessation of annual push moraine formation at the margin of Falljökull since 2004, coupled with the formation of "annual" meltwater channels and increased rate of ice-front retreat (of approximately 5 m/yr since 2005), has led *Bradwell et al*. [2013] to conclude that Virkisjökull-Falljökull has crossed a "glaciological threshold" leading to a marked change in its behavior. Since 2007, this twin outlet glacier has entered a phase of accelerated retreat and is retreating at a faster rate in any 5 year period since measurements began in 1932. Consequently, the glacier margin is no longer undergoing dynamic retreat but is now downwasting and collapsing through a range of geomorphological processes. The present multidisciplinary study has focused upon the structures developed within the marginal zone of Falljökull during this phase of collapse.

3. Methodology

[6] The present study of the deformation structures (fractures, faults) associated with the retreat of Falljökull comprises: (i) the initial terrestrial lidar scanning of the lower part of the glacier to provide a detailed Digital Elevation Model (DEM) of its surface, (ii) subsequent detailed structural study involving the mapping of the surface of the ice and analysis of exposed cliff sections through the glacier, accompanied by (iii) a Ground Penetrating Radar (GPR) survey to investigate the internal structure of the glacier and determination of ice thickness, and (iv) a second phase of lidar scanning. The initial phase of field work, involving lidar scanning of the ice, took place in September 2011. The structural glaciology study and GPR survey were carried out in a subsequent phase of field work in April 2012. A second lidar scan of the clean ice snout was obtained in September 2012.

3.1. Terrestrial Lidar Scanning of the Glacier

[7] Lidar scanning of Falljökull, using a Riegl LPM-i800HA medium- to long-range scanner, required multiple instrument setups at a series of locations around the glacier to minimize the number of "shadow areas" (areas obscured from the scanner's view) and obtain a complete surface model. Each component scan contained at least three common points to assist with orientation and significant overlap, typically around 10%. The different data sets were accurately referenced to a common coordinate system using a differential Global Navigation Satellite System (GNSS). A high-resolution digital camera mounted on the scanner allows the capture of colored "point-clouds," textured triangulated surfaces, or orthophotos with depth information. The lidar and GNSS data were processed to develop a Virtual Outcrop Model (VOM) of the glacier and its margin. Raw data produced by the RiPROFILE™ program consisted of point-clouds comprising 40 M x, y, z points for both lidar surveys. These data were oriented using the differential GPS positions and exported to an ASCII file comprising of x, y, z, intensity and RGB color values. The data were then imported into the "IMAlign" package within Polyworks (InnovMetrics™) to align individual scans and to check for errors in orientation. Surface 3D DEMs (see Figure 1c) were created using the "IMSurvey" package within Polyworks.

3.2. Structural Mapping and Analysis

[8] The large-scale pattern of fracturing within the relatively debris-free ("clean") ice within the marginal zone of Falljökull (Figure 1d) was established using the DEM of the glacier surface (Figure 1c) derived from the terrestrial lidar scanning and imported into an ArcGIS project. Although significant retreat and lowering of the glacier surface had occurred between September 2011 and April 2012, the main sets of structures developed within the ice could still be recognized, providing the focus for the later structural study. Structural mapping of a $30\,m \times 30\,m^2$ area of the surface of the ice, located close to the margin of the glacier and within a zone of intense ice deformation, involved the recording of the orientation (dip, strike, dip azimuth), sense and amount of offset (where applicable), and interrelationships between the various sets of faults, fractures, and foliations encountered along a series of 10 traverses, spaced at 3 m intervals (Figure 2a). Structural data were also obtained from a 275 m long traverse aligned parallel to the longitudinal axis of the glacier (Figure 2b). The location of this traverse coincided with profile F12-13 of the GPR survey (see below). The orientations of the planar structures identified on the glacier surface were measured using a compass clinometer (corrected for magnetic deviation) with the data being displayed on a series of lower hemisphere stereographic projections and rose diagrams (Figures 3a to 3h).

[9] The subsurface (internal) structural characteristics of the glacier were examined in a number of 5 to 15 m high ice-cliff sections located along southern and southeastern margins of Falljökull. Sequences of overlapping photographs were taken of these ice cliffs enabling the detailed analysis of the larger-scale structures developed along the entire length of the section. Particular emphasis was placed upon recording changes in the orientation of the faults, fractures and foliations, and the sense of movement on the faults, as well as the interrelationships between the various generations of structures allowing a detailed relative chronology of the ice deformation to be established (see below). The positions of englacial and subglacial drainage channels with respect to the larger deformation structures were also noted.

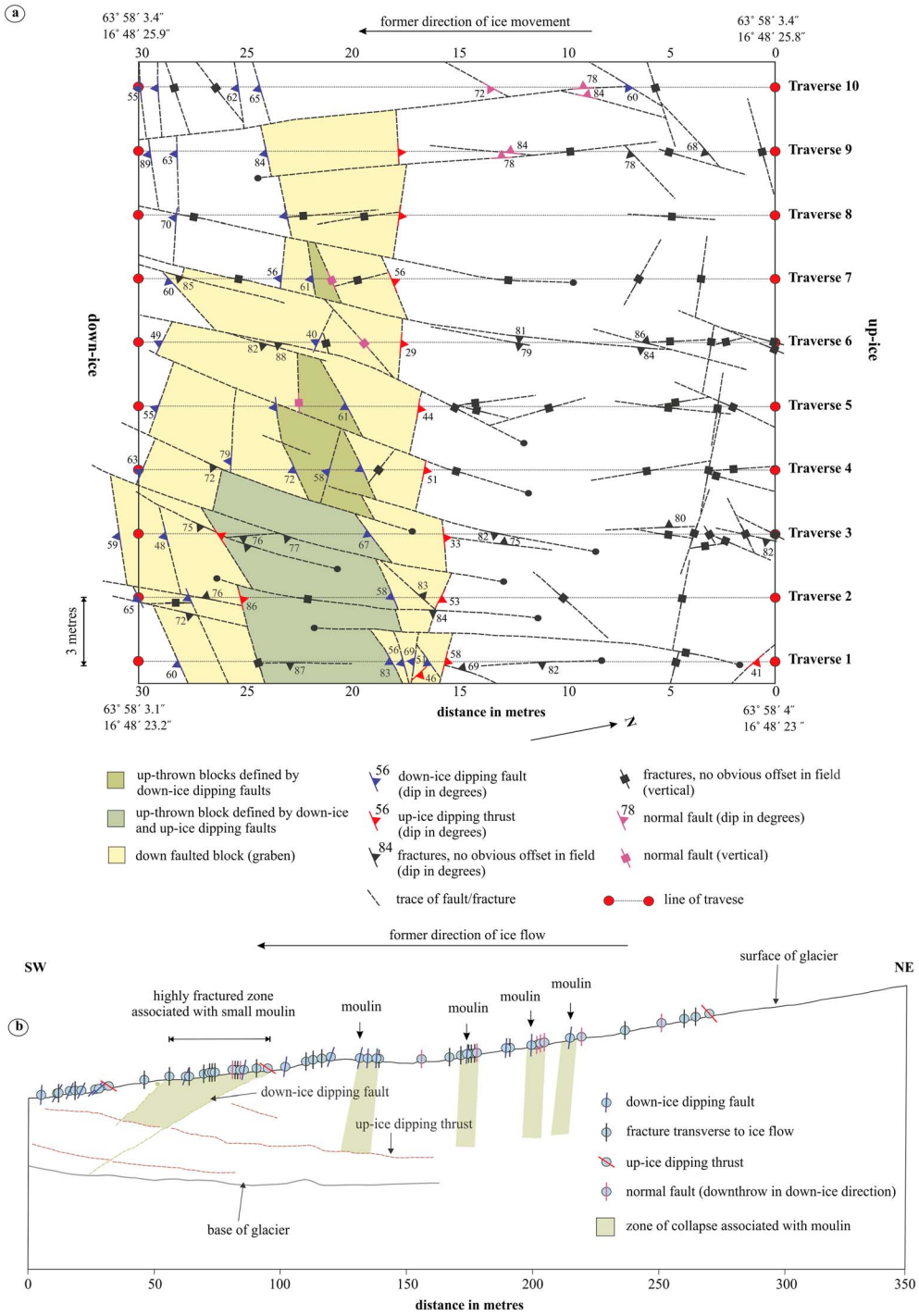

Figure 2. (a) Detailed structural map of the faults and fractures developed within a 30 m × 30 m^2 area on the surface of the ice close to the glacier margin. Note that the map includes part of a graben (shaded yellow) developed during collapse at the glacier margin; (b) Diagram showing the variation in the dip and relative density of the various fractures developed along an ice-flow parallel traverse along the axis of Falljökull. Also shown are the main thrust faults, down-ice dipping faults, and base of the glacier identified on the corresponding GPR section.

3.3. Ground Penetrating Radar (GPR) Survey

3.3.1. Data Capture and Processing

[10] GPR surveys have been successfully used to investigate glacier structure, since dielectric contrasts are produced by variations in water content and sediment content, and at the ice bed [*Arcone et al.*, 1995; *Hambrey et al.*, 2005; *Murray and Booth*, 2010; *Gusmeroli et al.*, 2012]. Common offset GPR surveys were conducted on the clean ice snout of Falljökull in April 2012 using a PulseEKKO Pro system with 50 MHz antennae. Four parallel 90 to 150 m long lines, positioned 10 to 20 m apart, were surveyed parallel to the direction of glacier flow (Figure 4a). Three 75

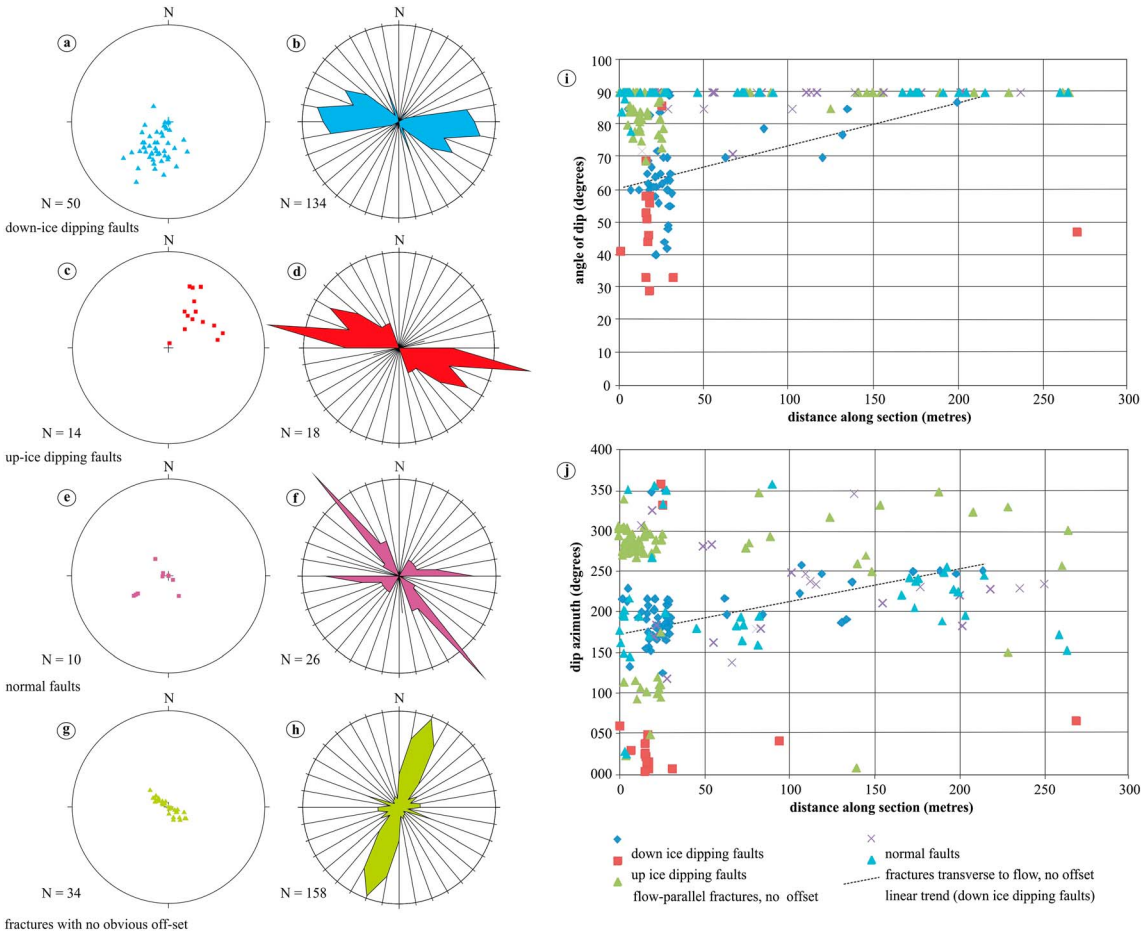

Figure 3. (a to h) Lower hemisphere stereographic plots of dip and dip azimuth, and rose diagrams of fracture trend for: (a and b) down-ice dipping faults; (c and d) up-ice dipping faults (thrusts); (e and f) normal faults; and (g and h) ice-flow parallel fractures. (i and j) Graphs showing variation in fracture and fault orientation with distance from the ice margin: (i) angle of dip versus distance along section; and (j) dip azimuth versus distance along section.

to 90 m long cross-glacier lines were also surveyed, spaced 30 to 40 m apart (Figure 4a). Antennae were positioned 2 m apart perpendicular to the line of survey, and moved manually at 0.5 m steps across the clean ice surface. Signals were stacked 128 times per trace, using a time window of 2000 ns and a sampling interval of 1600 ps. A standalone Novatel SMART-V1 GPS antenna, with ~1.8 m positional accuracy, was fitted to the rucksack of the control unit operator. Raw GPR data were processed in EKKO View Deluxe [*Sensors and Software*, 2003]. Processing primarily consisted of applying a dewow filter, band-pass filtering, 2D migration, and topographic correction. Water content in temperate glaciers reduces the velocity of radar propagation relative to that of cold glacier ice. A radar wave velocity of 0.156 m ns^{-1}, previously calculated for Falljökull by *Murray et al*. [2000], was used for processing and interpretation of the profiles. Analysis of hyperbola in unmigrated profiles supported the use of this velocity.

3.3.2. Subsurface 3D Modeling

[11] Interpretation of subsurface glacier structure was carried out using the geological modeling package, GOCAD^{TM}. Key reflectors were picked allowing a skeleton network of subsurface structures to be identified (Figures 4b and 4c). Combining this network with the surface structural measurements (Figures 2 and 3) allowed a control data set to be created, from which glacier structures were interpolated using a Discrete Smooth Interpolation method [*Mallet*, 1997] (Figure 4d).

4. Structural Mapping of the Surface of the Glacier and Analysis of Ice Cliffs

4.1. Faults and Fractures

[12] A map of the brittle deformation structures present within the debris-free central section of Falljökull is illustrated in Figure 1d. Two principal fracture sets have been identified:

[13] 1. A set of vertical to subvertical, closed fractures which typically exhibit very little or no displacement, and are orientated (trend) parallel to the former ice flow direction of the glacier. These laterally extensive fractures have been identified along the entire length of the glacier from the ice fall to its snout;

[14] 2. A complex set of faults and fractures occurring approximately orthogonal to the axis of the glacier. These structures form discrete zones of relatively more intense brittle deformation (green-shaded areas on Figure 1d).

[15] The number and density of the crosscutting faults and fractures increase toward the glacier margin, indicating

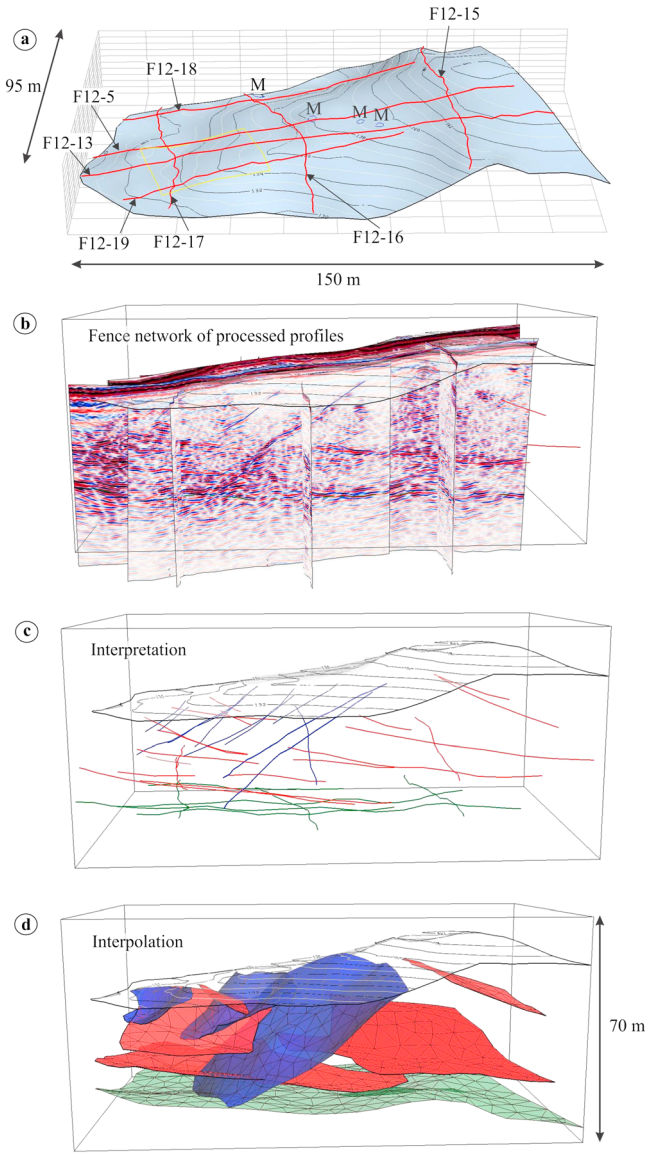

Figure 4. (a) Position of GPR survey lines (red) on the clean ice margin of Falljökull. M denotes the position of the moulins; (b) Fence network of processed survey lines; (c) 3D image showing main reflectors picked from survey lines; (d) Interpolation of reflectors (combined with surface observations) to reveal interpreted internal glacier structure.

that their development is related to deformation occurring within this marginal zone. In detail, the crosscutting structures can be subdivided into four subsets (see Figures 2, 3, and 5): First, a set of moderate to steeply inclined (40° to 90°), down-ice dipping normal (extensional) and reverse (compressional) faults. Displacement on these faults ranges up to 70 cm, with a number of individual faults showing a pronounced displacement gradient (down to 0 cm) toward their tips; A second set of shallowly to steeply (28° to 85°, typically below 60°) up-ice dipping reverse faults and thrusts with a sense of displacement toward the S/SW; Third, a variably developed conjugate set of steeply inclined (70° to 90°) normal faults; And finally a set of fractures transverse to the former direction of ice flow, but which exhibit no visible offset. The exposed surfaces of all the fault sets, although gently undulating, are smooth with no obvious striae or slickensides.

[16] Orientation data obtained for these structures are displayed graphically in Figures 2 and 3. Examples of the faults, as well as ice-flow parallel fractures, are shown in Figure 5. The data reveal that the angle of dip of fault set 1 becomes progressively shallower toward the ice margin (Figures 2b and 3i), accompanied by an anticlockwise rotation (10° to 15° toward the south) in the dip azimuth for all four fault/fracture sets (Figure 3j). A similar southerly directed (anticlockwise) rotation is also observed in the trend (strike) of the ice-flow parallel fractures (compare data from Zones 1, 2, and 3 on Figure 1d). This progressive change in orientation of the brittle deformation structures in the lower part of Falljökull potentially records a systematic change in the orientation of the principal stress axes, reflecting a change in the stress regime due to the interaction between Falljökull and Virkisjökull downstream of Rauðikambur (see Figure 1b).

[17] The zones of relatively intense brittle fracturing and faulting which crosscut the glacier take the form of 5 to 30 m wide down-faulted blocks, or graben, bounded by prominent up-ice and down-ice dipping faults (Figure 6a). In total, three such zones have been identified within the lower part of Falljökull (Figure 1d). The down-ice dipping reverse faults which bound down-ice margins of the graben are open structures with extension occurring across the fault leading to the opening of up to 10 to 15 cm wide void/aperture along parts of the fault plane. Thin (up to 10 cm thick) "aprons" of fine-grained sand and silt are locally developed immediately adjacent to these faults (Figure 5a). This relationship is consistent with the sediment having been "expelled" or "evacuated" onto the glacier surface via these faults, probably during faulting, facilitated by extension occurring across these down-ice dipping structures. In April 2012, the planes of the exposed down-ice (Figure 5b) and up-ice dipping faults (Figure 5c), as well as the associated fault scarps, exhibited very little or no evidence of degradation due to surface melting.

[18] Detailed mapping of part of the surface of Falljökull has revealed that the graben are internally complex, comprising an assemblage of up-thrown and down-faulted blocks (Figures 2a and 6a). This pattern of faulting/fracturing, coupled with differential weathering along these brittle fractures near the margin of the glacier, results in a distinctive blocky, "chocolate bar"-like, appearance to the glacier surface (Figure 5b). Although the fractures developed parallel to the former ice flow direction typically show very little evidence of having accommodated any movement, within the graben vertical dip-slip or oblique-slip movement, resulting in displacements of between 10 to 20 cm, have been recorded on some fractures (Figure 5d). Furthermore, this movement led to the variable offset of the down-ice and up-ice-dipping faults which are reorientated across the ice-flow parallel structures (see Figure 2a).

4.2. Moulin

[19] Figure 1d shows that the moulins in the lower part of Falljökull are spatially related to zones of relatively more intense brittle deformation which crosscut the glacier. The moulins occur at the intersections between prominent down-ice dipping faults and several closely spaced ice-flow parallel fractures (Figures 6b, 6c, 6d, and 6e). Three small

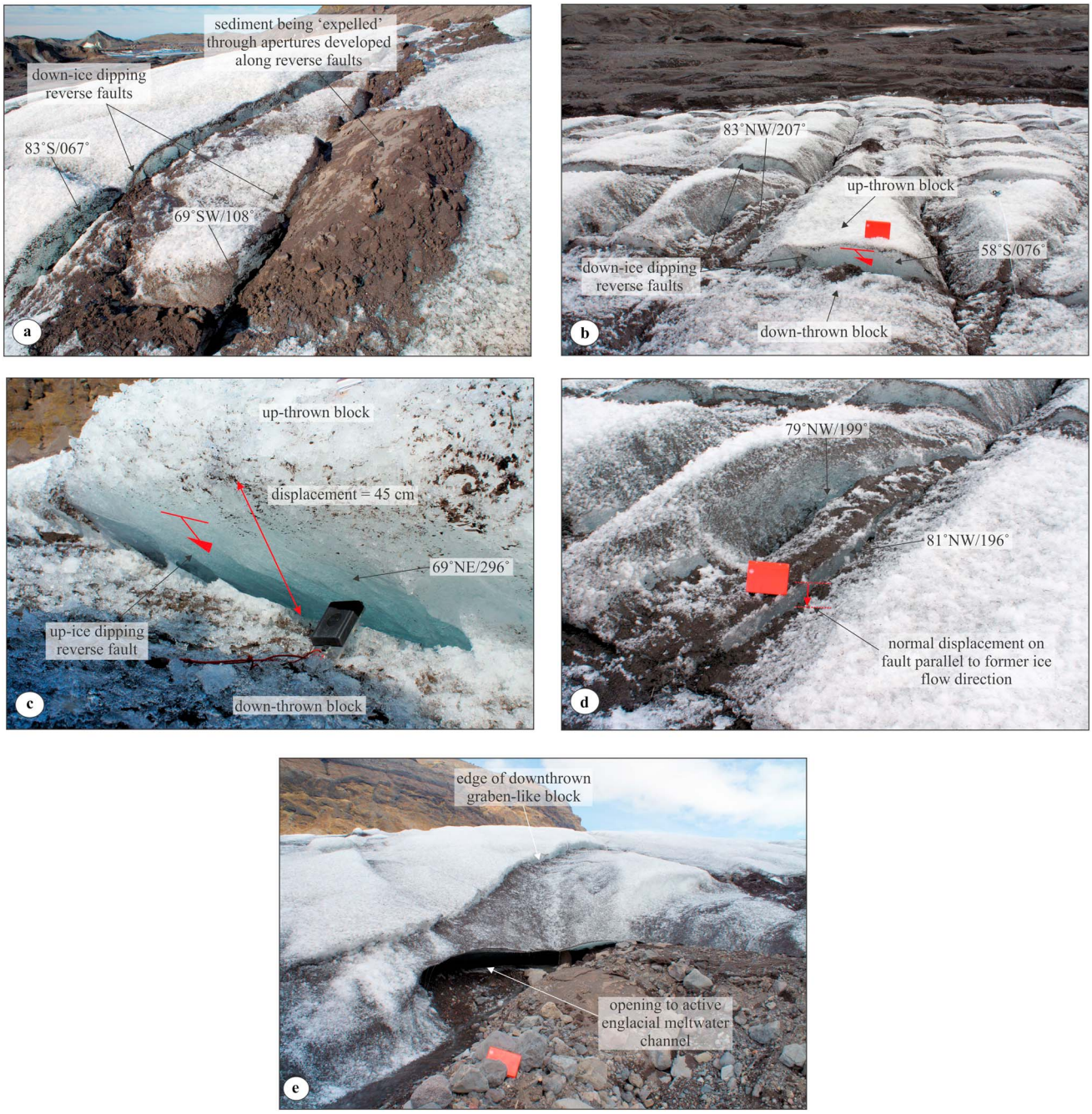

Figure 5. (a) Down-ice dipping faults with recently formed angular fault scarps recording a reverse sense of movement. Also note that the thin "aprons" of sediment on the glacier surface associated with these structures; (b) "Chocolate bar" style of block faulting near the margin of the glacier formed by the intersection of down-ice dipping faults and ice-flow parallel fractures; (c) Exposed fault plane of an up-ice dipping reverse fault due to recent movement (winter 2011–2012); (d) Normal sense of displacement on an ice-flow parallel fracture; (e) Opening to an active englacial channel emerging from beneath the margin of a graben.

moulins (openings on the surface of c. 50 cm in diameter), located in the center of the study area (Zone 2, Figure 1d), occur within a shallow, dish-shaped depression of relatively intense block faulting/fracturing (Figure 6b). The moulins in this area form roughly cylindrical, moderately to steeply inclined (50° to 70°), down-ice dipping features which follow the planes of down-ice dipping faults. In detail, the moulins are located at the intersections between the faults and the ice-flow parallel fractures (Figures 6b and 6c).

[20] A large moulin located on the western side of the glacier (Zone 2, Figure 1d) shows a similar relationship to the down-ice dipping faults, occurring within a prominent, 10 to 15 m wide fault zone comprising several, closely spaced, locally crosscutting, normal and reverse structures (Figure 6d). These active faults are marked by angular scarps on the glacier surface, with the latest phase of brittle reverse movement having accommodated displacements of up to 25 to 30 cm (Figure 9b). Surface examination of the moulin

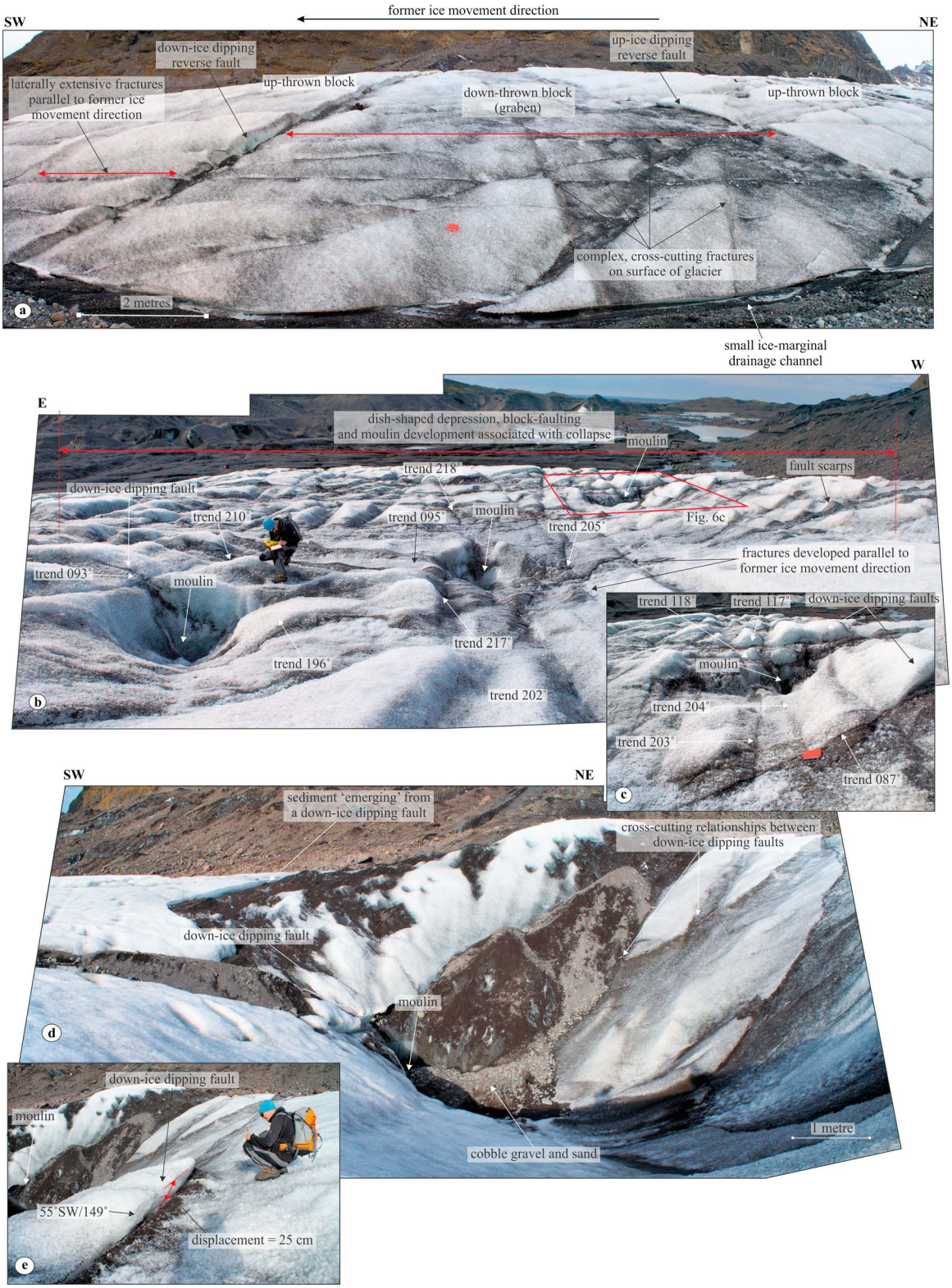

Figure 6. (a) A fault-bound, 10 to 15 m wide, down-thrown block of ice (graben) developed near the margin of Falljökull. Note the complex pattern of crosscutting faults and fractures within the graben; (b) Openings to three small moulin developed within a dish-shaped depression within the surface of Falljökull; (c) Photograph showing that the moulin is developed at the intersection between the down-ice dipping faults and the ice-flow parallel fractures; (d) Large depression formed around a prominent moulin developed on the western side of Falljökull. The moulin is developed within a wide fault zone composed of crosscutting, down-ice dipping structures (see text for details); (e) Angular fault scar marking a down-ice dipping fault recording a reverse sense of movement.

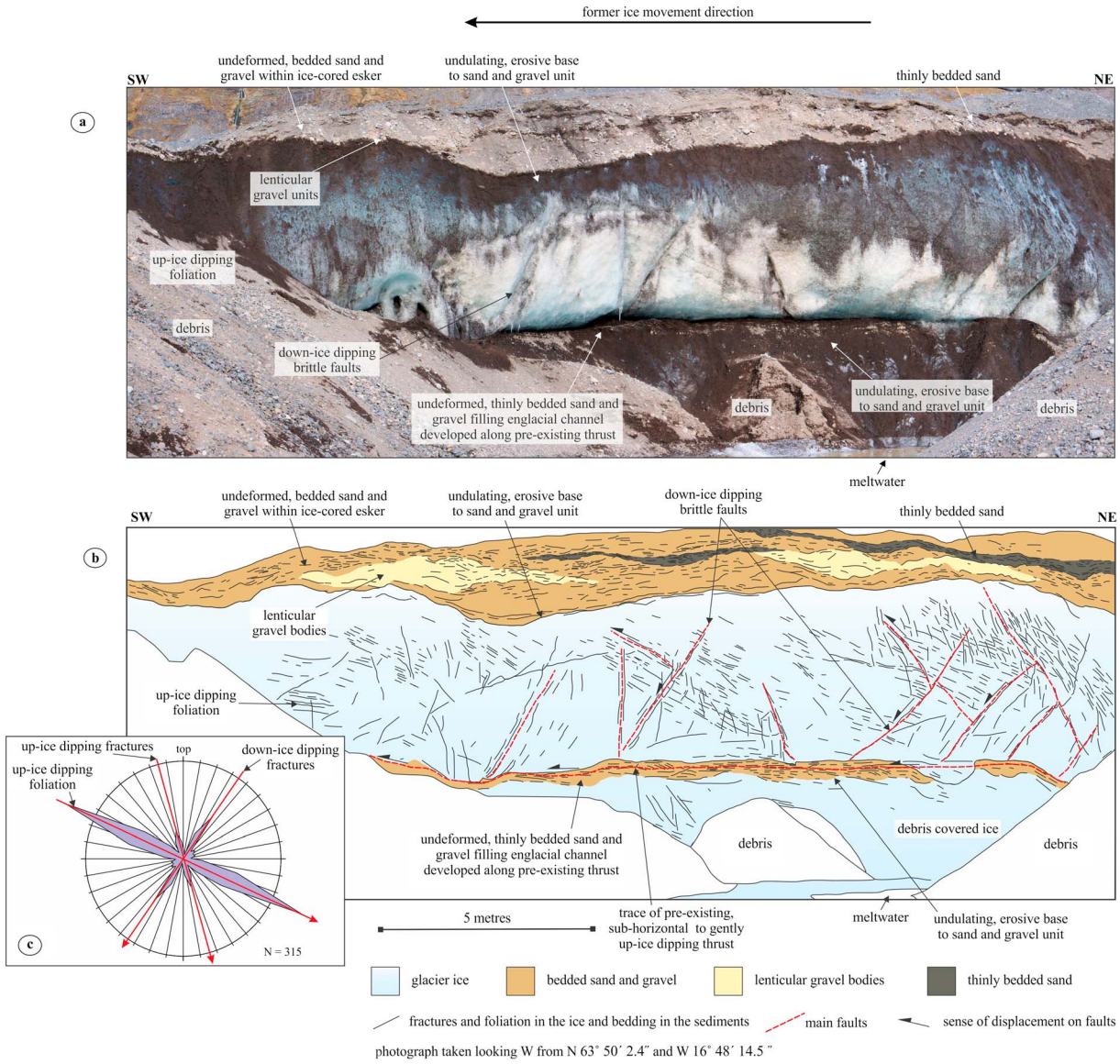

Figure 7. (a) Photomontage of an ice-cliff section 1 exposed within the ice-cored esker (see Figure 1b); (b) Interpretation diagram showing the relationships between a well-developed foliation within the ice and the crosscutting faults and fractures (vertical = horizontal scale); (c) Rose diagram showing the angle of dip of the foliation and fractures.

indicates that it forms a pipe-like feature which follows the fault zone. The sound of fast flowing water could be heard from the surface, indicating that the moulin is connected to an active englacial meltwater channel at depth. However, in April 2012, there was no evidence of surface drainage running into any of the moulins present within the marginal zone of Falljökull.

4.3. Ice-Cliff Sections

[21] A number of steeply inclined to subvertical ice-cliff sections (5 to 15 m high) along the southern and southeastern margin of Falljökull have allowed the subsurface (internal) structure of the glacier to be investigated. Four examples of these ice-cliff sections are illustrated in Figures 7 to 9.

[22] The first example, section 1 (Figure 7), occurs through ice proximal end of a prominent ice-cored esker revealed during the retreat of the margin of Falljökull (see Figure 1b). This esker marks the position of a former englacial (major) drainage channel [*Bradwell et al.*, 2013] and comprises a relatively thin (0.5 to 2 m thick) sequence of bedded sands and gravels overlying 5 to 6 m of foliated ice (Figure 7). The foliation within the ice dips at c. 25° toward the northeast and is offset by a number of moderately to steeply inclined (50° to 60°) down-ice dipping normal faults. The faults terminate at, or transfer, into a prominent subhorizontal detachment (thrust) marked by a laterally discontinuous layer of undeformed, thinly bedded sand and gravel (Figure 7). The top of this layer of sediment is sharp and planar in form. However, its base is irregular, consistent with these bedded sediments having been deposited by fast flowing meltwater flowing along the preexisting thrust and eroding into the underlying ice. A small number of moderately to steeply inclined up-ice dipping fractures have also been recognized within this section.

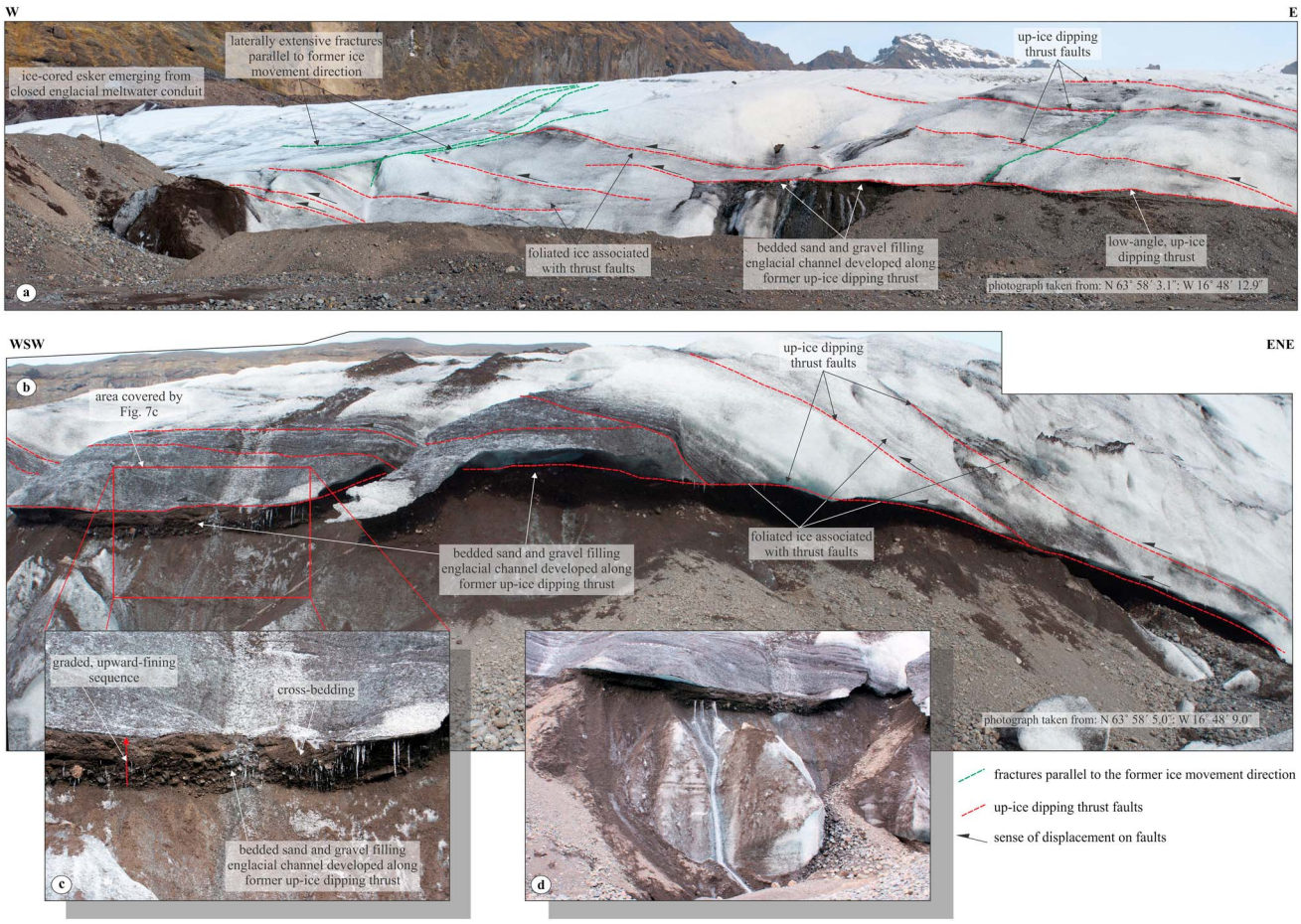

Figure 8. (a) Photomontage of section 2 through the clean ice margin of Falljökull (see Figure 1b) showing the imbrication and stacking of thrust-bound slices of foliated ice; (b) Photomontage of an ice-cliff section 3 located to the west of the main meltwater outlet draining Falljökull. Note the presence of a layer of bedded sand and gravel marking the line of a prominent, gently up-ice dipping décollement (thrust); (c) Details of undeformed, well-bedded sand and gravel layer present along up-ice dipping thrust. These waterlain sediments are graded from a cobble gravel at the base to cross-bedded sand at the top; (d) Meltwater flowing out of the sediment layer developed along a preexisting thrust showing that these sediment-lined structures continue to act as a fluid pathway through the ice.

[23] Sections 2 (Figure 8a) and 3 (Figure 8b) are located within the clean, debris-free ice at the front of the glacier (Figure 1b), to the west of the main meltwater outflow conduit, and reveal that it is deformed by a number of low-angle, up-ice dipping, S/SE-directed thrusts which link into a prominent, gently up-ice dipping detachment. The thrusts occur within, or cut through a 5 to 10 m thick zone of foliated ice (Figures 8a and 8b) and can be traced laterally (westward) across the front of the glacier where they form the up-ice margins of the graben. The foliation within the ice is clearly truncated and offset by the thrusts and the associated large-scale detachment (Figure 8b), indicating that brittle thrusting largely postdated the imposition of this ductile fabric. The large-scale detachment seen in section 3 is marked by a series of elongate lenses of bedded sand and gravel which show very little evidence of glacitectonic disturbance (Figures 8b, 8c, and 8d). These waterlain sediments comprise an upward fining sequence (up to 70 to 80 cm thick) with a distinct gravel base overlain by parallel-bedded to cross-bedded sand (Figure 8c). At the start of field work, the sediments were dry or frozen (Figure 8c). A few days later, however, meltwater was clearly flowing through these deposits (Figure 8d), indicating that such sedimentary layers may act as fluid (meltwater) pathways through the ice.

[24] Section 4 (Figure 9) occurs through the debris-covered ice on the southeastern side of Falljökull (see Figure 1d) and reveals a thick unit (several meters thick) of apparently darker, foliated ice at the base of the glacier directly overlying the volcanic bedrock. This foliated basal ice is deformed by a series of low-angle thrusts which link into a number of prominent subhorizontal detachments (thrusts) (Figures 9a and 9b). These detachments are once again locally marked by lenses of thinly bedded sand and gravel which show very little or no evidence of deformation. Imbrication and stacking of thrust-bound slices of foliated ice are revealed by systematic changes in the apparent dip of this fabric (Figure 9c). Crosscutting relationships observed between the thrusts indicates that the glacier has accommodated several phases of thrusting. However, the sense of offset of the foliation across the thrusts records a consistent S/SE-directed sense

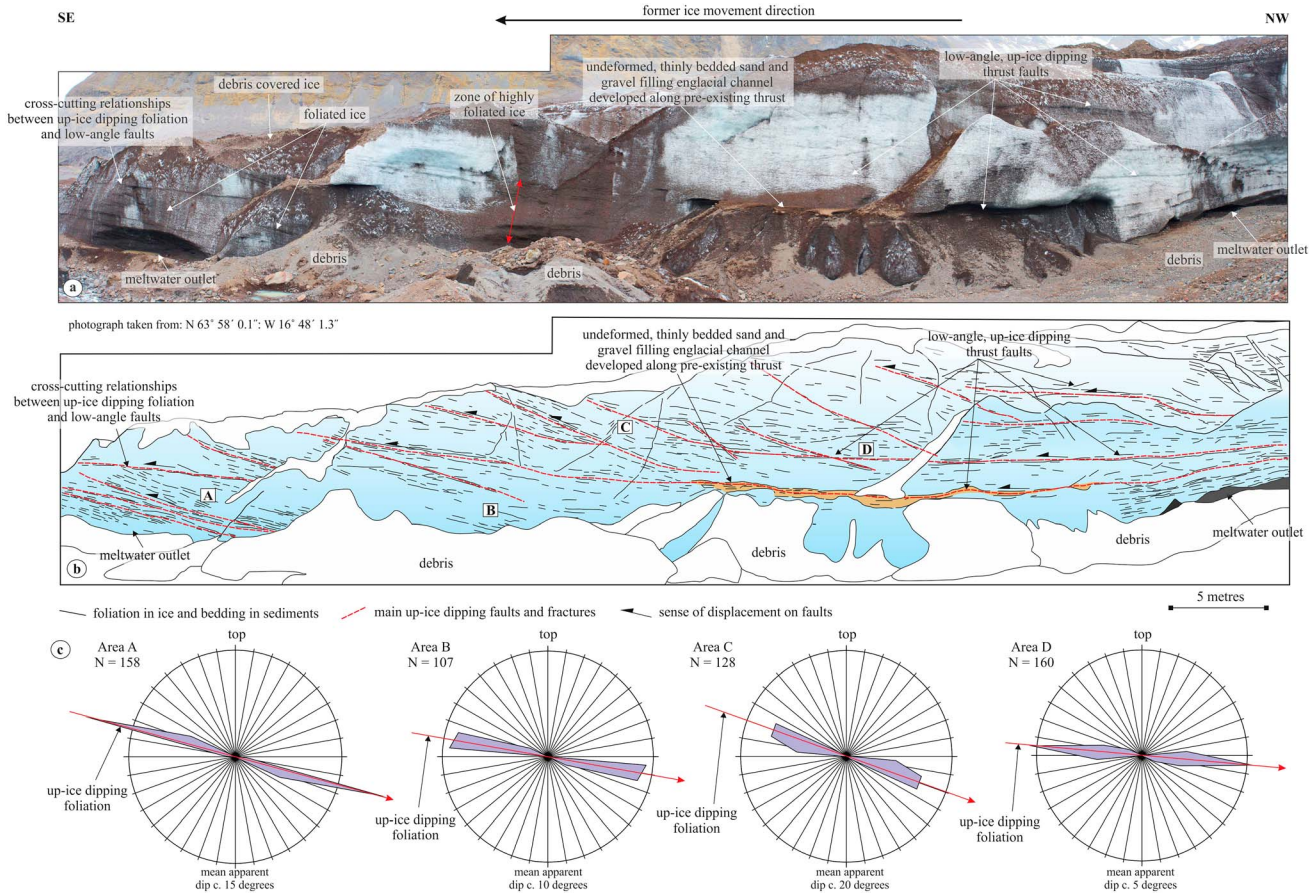

Figure 9. (a) Photomontage of an ice-cliff section 4 located on the eastern margin of Falljökull (see Figure 1b) showing the structures developed within the debris-covered ice; (b) Interpretation diagram showing the relationships between a well-developed foliation within the ice and the crosscutting faults and fractures (vertical = horizontal scale). The crosscutting relationships between the faults clearly indicate that the ice has accommodated several phases of S/SE-directed thrusting; (c) Rose diagram showing the variation in the angle of dip of the up-ice dipping foliation across the section.

of movement, indicating that these repeated phases of thrusting probably accompanied the forward motion of the glacier (also toward the S/SE).

[25] No evidence of the down-ice dipping faults observed in section 1 (Figure 7) and graben-like structures (Figures 2a and 6a) identified during the surface mapping of Falljökull (Figure 7) have been identified in sections 2, 3 or 4 (see Figures 8 and 9), suggesting that this style of deformation was restricted in its occurrence.

5. 3D Subsurface Structure of the Glacier

[26] The GPR profiles show a degree of background scatter, typical of temperate glacier ice [*Navarro et al.*, 2005; *Woodward and Burke*, 2007; *Gusmeroli et al.*, 2012]. However, strong reflectors are present and can be divided into three types: (i) a basal, often laterally continuous, subhorizontal reflector (Figure 10a), (ii) shallow up-ice dipping reflectors (Figure 10b), and (iii) steeper down-ice dipping reflectors (Figure 10c).

[27] The basal, reverse phase reflector is generally continuous, but in places its reflectivity is masked by reflectors at higher elevations. In profiles F12-18 and F12-5, this basal reflector is generally flat lying at an elevation of approximately 96 m, with gentle undulations. In profiles F12-13 and F12-19, it dips gently up-ice, descending at ~5° from ~100 m to ~96 m before leveling out farther up-glacier. In the three cross-glacier profiles, the basal reflector slopes very gently toward the northwest at angles of 0° to 4°. This generally flat lying basal reflector is interpreted as the glacier bed. Observations from the valley sides at the margins of Falljökull show that the glacier snout rests on a thin (generally < 1 m), discontinuous subglacial till, which overlies semilithified volcanogenic diamicton. In the study area, near the valley center, glacier ice thickness is ~40 m at the transition from the sloping clean ice margin to nearly flat lying, gravelly sandy outwash, highlighting the thickness of buried glacier ice that is present in front of the clean ice margin.

[28] In the longitudinal GPR profiles, the up-ice dipping reflectors (T1–T4) show a variety of dips, from subhorizontal to 20° (Figure 11). In general, these reflectors become steeper near the glacier surface, and also in a down-ice direction. The cross-glacier profile F12-15 (see Figure 4a) also shows that at least one of these reflectors has a cross-glacier dip toward the southeast (Figure 11). The geometry of these up-ice dipping reflectors is consistent with the interpretation that they represent englacial thrust planes; their presence within Falljökull is confirmed by the ice-cliff sections which show a similar geometry (see section 4.3).

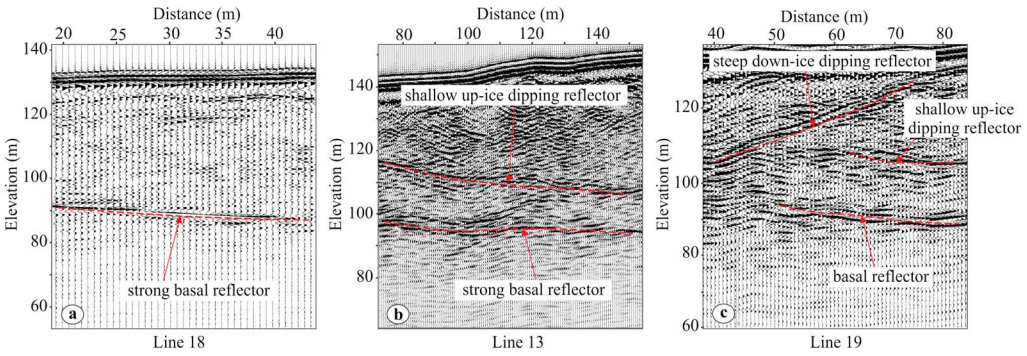

Figure 10. Extracts from processed GPR survey lines, showing examples of: (a) a strong, continuous, subhorizontal basal reflector; (b) a shallow up-ice dipping reflector; (c) a steeper down-ice dipping reflector.

[29] The steeper down-ice dipping reflectors are interpreted as fault planes. These faults intersect the zones of lateral fractures that were recorded on the ice surface (see section 4.1.). The down-ice dipping reflectors (F1–F3, Figure 11) dip at angles of between 25° and 35°, becoming shallower in a down-ice direction. A major down-ice dipping reflector (F1, Figure 11) can be seen to extend from the surface of Falljökull, down to the subhorizontal reflector marking the base of the glacier. This prominent down-ice dipping reflector crosscuts and appears to offset one of the up-ice dipping reflectors (T2, Figure 11), indicating that this F1 feature represents a major fault which postdated the earlier T2 thrust. The down-ice dipping reflectors F2 and F3 extend at least ~15 m below the glacier surface, but become harder to trace within a zone showing a high amount of scatter. These relationships are consistent with the down-ice dipping reflectors representing smaller-scale normal and reverse faults identified during the surface mapping of Falljökull (see section 4.2). The location of the F2 and F3 reflectors indicates that they represents the bounding faults of one of the down-faulted graben (Figures 12a and 12b) identified on the surface of Falljökull.

[30] Interpolation of the various reflectors together with the observed surface fractures and faults has allowed a detailed three-dimensional model of the clean glacier snout to be constructed (Figure 12c). The characteristics of the model and the surface structural observations are discussed below in relation to the recent evolution of the glacier structure.

6. Glacier Deformation During Ice-Margin Collapse and Retreat

6.1. Ice Deformation History and Model of Ice-Margin Collapse

[31] Crosscutting relationships between the various structures (faults, foliations, fractures) allow the deformation history recorded by Falljökull to be divided into three main phases:

[32] 1. **Phase 1** – an early phase of predominantly ductile deformation leading to the development of a gently up-ice dipping to subhorizontal foliation within the lower part of the glacier;

[33] 2. **Phase 2** – a phase of S/SE-directed brittle thrusting which resulted in the stacking of fault-bound slices of ice, possibly leading to glacitectonic thickening of the glacier;

[34] 3. **Phase 3** – late stage brittle faulting (normal and reverse), fracturing, and graben development within the marginal zone of the debris-free ice which forms the central corridor of Falljökull.

[35] The development of a foliation within the ice and subsequent S/SE-directed thrusting is consistent with Phases 1 and 2 of the deformation history having accommodated compressional deformation resulting from the forward movement (advance) of the glacier. Structures associated with these early phases of deformation are best preserved/exposed within the debris-covered ice along the eastern margin of the glacier. The main up-ice dipping thrust faults/detachments within the glacier are clearly identified by the GPR survey (Figures 11 and 12), showing that they are laterally extensive structures consistent with their formation in response to the forward motion of Falljökull rather than collapse at the ice margin. The flow-parallel fractures which have been identified along the entire length of the glacier from the ice fall to its snout are also thought to have developed during the earlier stages of the deformation history.

[36] Unlike the earlier thrust-dominated deformation of Phase 2, brittle deformation during Phase 3 was spatially constrained to the marginal zone of the glacier, consistent with this stage of deformation history leading to the collapse and retreat of the ice margin. Field evidence (e.g., displacements on exposed fault planes) from the clean ice in the marginal zone of Falljökull clearly indicates that this phase of deformation is still ongoing. In April 2012, the exposed fault scarps (Figures 5a, 5b, 5c, and 6) exhibited very little or no evidence of degradation due to surface melting. This evidence suggests that movement on the faults (displacements up to

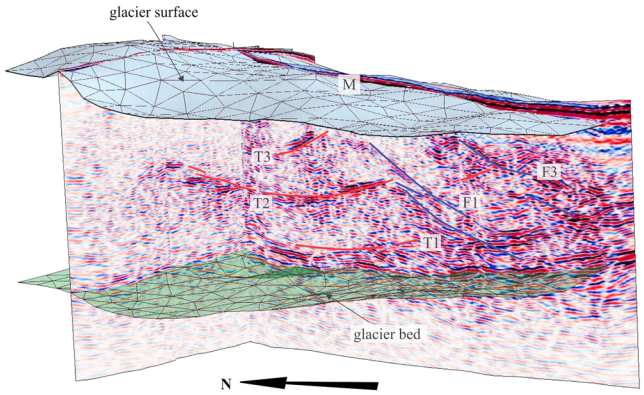

Figure 11. 3D conceptual model showing the internal geometry of the clean ice-margin area of Falljökull. The positions of the major up-ice dipping thrusts (T1 to T3) and main down-ice dipping faults (F1 and F3) are also shown.

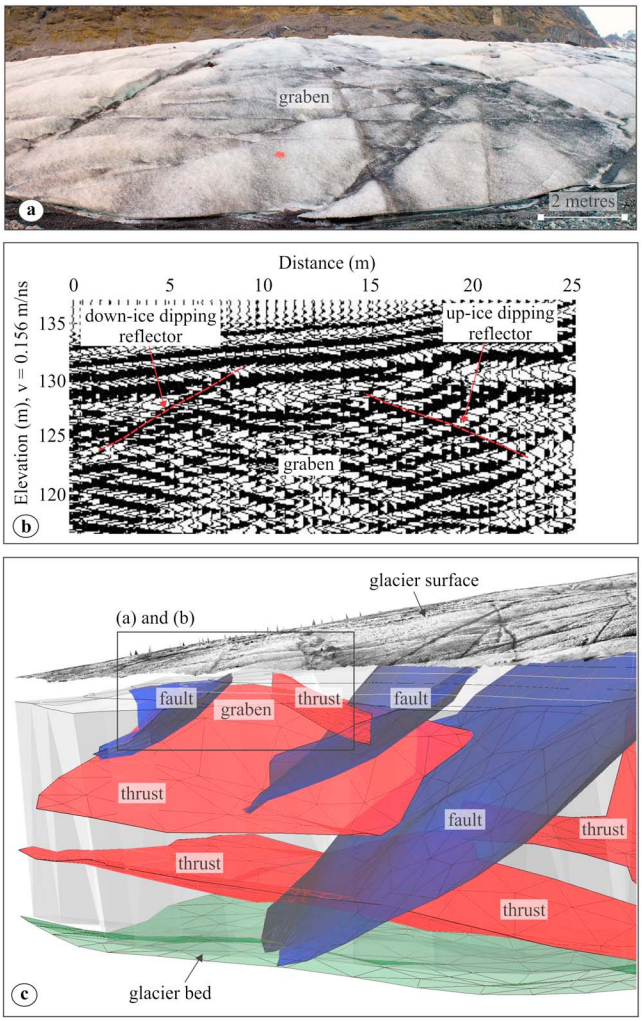

Figure 12. Down-faulted graben structure. (a) Photograph showing graben as represented at the glacier surface; (b) GPR data show up-ice and down-ice dipping reflectors associated with the graben; (c) Graben within the wider interpreted context of the subsurface structure at the margin of Falljökull.

70 cm), leading to the observed offset of the glacier surface, probably occurred during the previous (2011–2012) winter.

[37] Any conceptual model of active, collapse-related deformation at the margin of Falljökull needs to account for the following:

[38] 1. The overall increase in intensity of faulting and fracturing toward the margin;

[39] 2. The observed decrease in the angle of dip of down-ice dipping faults toward the margin;

[40] 3. The apparent steepening of up-ice dipping thrusts toward the ice margin and toward the glacier surface;

[41] 4. The development of discrete zones of relatively more intense brittle deformation orthogonal to the axis of the glacier;

[42] 5. The complex, "chocolate bar" pattern of fracturing and faulting within these highly deformed zones;

[43] 6. The development of down-faulted, graben-like features which are typically equated with compressional deformation within a zone undergoing extensional collapse; and

[44] 7. The step-like morphology of the surface of the glacier within its marginal zone.

[45] The simplest interpretation of the deformation structures within the marginal zone of the glacier is in terms of a block rotation occurring in response to movement on the steeply inclined, down-ice dipping normal faults (Figure 13). GPR data indicate that these faults are listric in nature (Figures 11 and 12c), i.e., steeply inclined near the surface of the glacier, but becoming more shallowly dipping downward where they link into, or terminate at, the major thrusts and/or glacier bed (see Figures 12c and 14). They are not composed of a single fault plane, but comprise a complex zone of closely spaced brittle faults and fractures. The intersection of these fault systems with the upper surface of Falljökull are marked by the zones of more intense brittle deformation (green shaded areas on Figure 2). The complex "chocolate bar" pattern of faulting and fracturing within these zones (Figures 5c and 6a and 6b), which includes both normal and reverse faults, probably occurred in response to differential movement on the individual structures as they accommodated the overall extensional displacements across the much wider normal fault zones. Furthermore, block faulting, differential collapse, and the associated areal subsidence within the normal fault zones would also lead to the observed increase in surface loss in the immediate footwall of these extensional structures (see Figure 14). Consequently, surface mass loss within the marginal zone of Falljökull can be considered to be a direct result of both surface ablation and structural controlled collapse (see section 6.3).

[46] The increase in intensity of brittle deformation toward the margin of Falljökull has led to the conclusion that the down-ice dipping normal fault zones are the main structures controlling glacier margin collapse. The overall geometry of this style of collapse is reminiscent of multiple rotational slope failures in mud-rich bedrock/sediments (Figure 13a) [*Waltham*, 2010] where the failure is achieved along listric or curved slip surfaces (faults). The position of the "headwall" of this multiple slope failure will migrate progressively up-ice as the glacier retreats. Consequently, Phase 3 deformation is diachronous, becoming progressively younger in an up-ice direction. The listric nature of the faults leads to the hanging-wall blocks undergoing passive rotation and tilting during failure (Figure 13c). As a consequence of the rotation of these fault blocks, any preexisting glaciological structures will be reorientated. This would lead to the observed decrease in the angle of dip of down-ice dipping faults toward the glacier margin and simultaneous back-rotation and steepening of the up-ice dipping thrusts. Rotation of the individual fault blocks would also result in a marked lowering of the glacier surface immediately adjacent to the fault, effectively increasing the amount of surface loss on its down-throw side. Simultaneously the down-ice end of the fault block is undergoing relative uplift (Figure 13c); the latter potentially offsetting the effects of surface ablation or even leading to net gain in this area. Rotational tilting of the fault blocks within the proposed multiple rotational failure would result in the step-like surface morphology observed within the marginal zone of Falljökull. Continued ablation during the summer months will "smooth out" this structurally induced surface topography; shown by lines 1, 2, and 3 on Figure 13c.

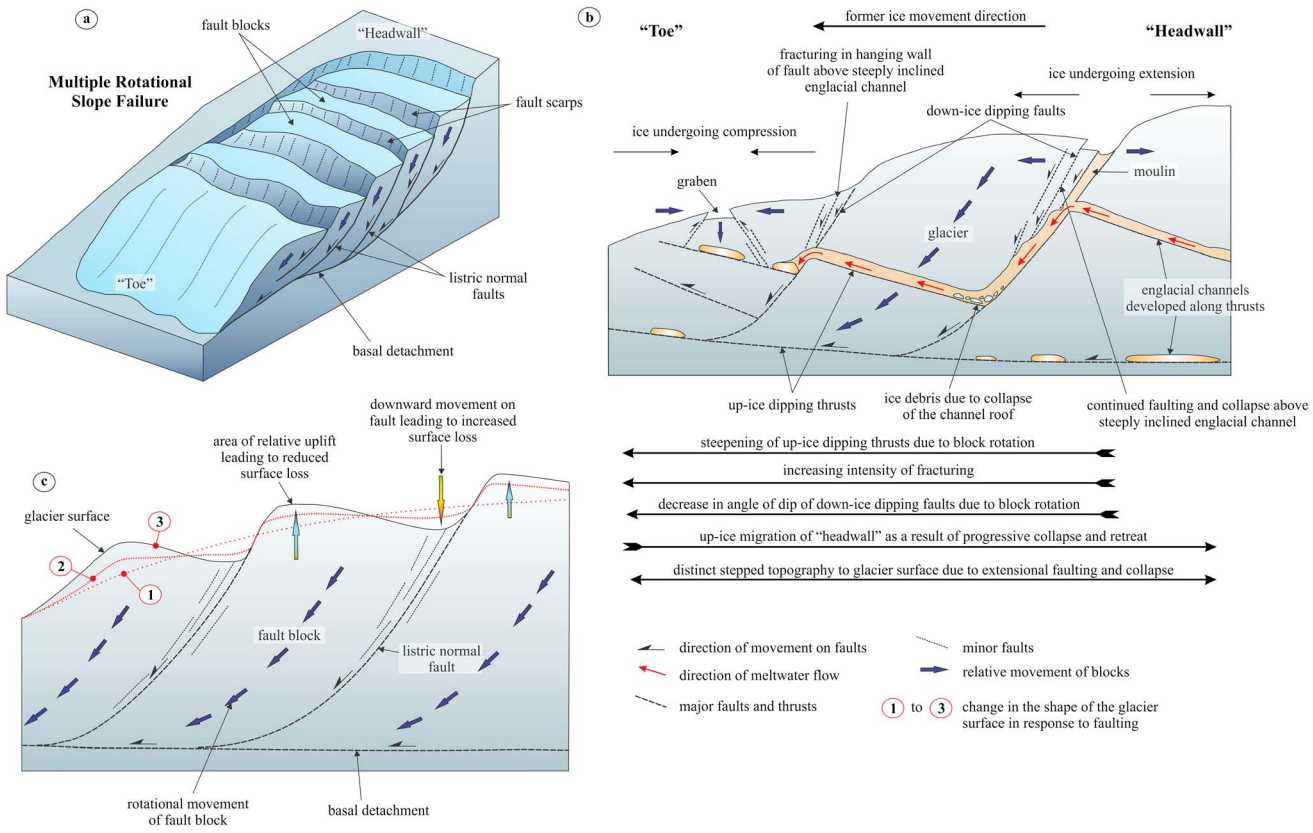

Figure 13. (a) Conceptual model for the collapse of the clean ice at the margin of Falljökull in response to multiple rotational slope failure; (b) Schematic cross section through the clean ice at the margin of Falljökull showing the relationships between faulting, the pattern of englacial drainage, and moulin development during the ice-margin collapse; (c) Schematic cross section through the clean ice at the margin of Falljökull showing the potential relationship between faulting and changes in the surface of the glacier (see text for details).

[47] Movement at the "toe" of the multiple slope failure at the margin of Falljökull appears to be "pinned" by the buried ice underlying the proglacial outwash. This static ice is effectively acting as a "buffer" limiting forward motion of the collapsing fault blocks, leading to compression within the ice at the "toe" as the glacier accommodates movement resulting from continued collapse further up-ice. This compressional deformation is responsible for the development of the graben-like structures which accommodated shortening within the lower part of the glacier (Figures 12 and 13). The down-ice margins of the graben are controlled by down-ice dipping reverse faults (see Figures 6a, 12a and 12b). These structures formed in response to the reactivation (inversion) of preexisting down-ice dipping normal faults. Back-rotated (steepened), Phase 2 thrust faults which form the up-ice margin of the graben (Figure 12) are similarly reactivated as deformation within the ice changed from initially extensional during the earlier stages of collapse, to compressional as the rotating fault block moves toward the "toe" (Figure 13b). Collapse within the graben may be locally facilitated by the presence of englacial drainage channels beneath the down-faulted block (Figures 5e and 13b). During periods of low flow, such channels will empty leaving an open cavity which can accommodate further movement on the bounding faults, effectively "undermining" the down-faulted block and accelerating its collapse (see Figure 13b).

6.2. Model for Moulin Development in Response to Collapse

[48] It is clear from Figure 1d that the moulins within the marginal zone of Falljökull show a close spatial relationship to the zones of intense (Phase 3) brittle deformation, indicating that there may be a link between moulin formation and structural changes to the glacier in response to collapse of its margin. In April 2012, there was no, or very little, evidence for any significant supraglacial drainage having fed into the moulins (see Figures 6b to 6d). However, fast flowing meltwater could be heard at depth, indicating that the moulin was connected to active englacial drainage channels. The lack of surface drainage associated with the moulins at Falljökull is in marked contrast with published models for moulin development which involve their formation at the point where supraglacial drainage channels penetrate the glacier surface, linking these surface streams with englacial or subglacial drainage systems [see *Benn and Evans*, 2010, and references therein]. Detailed structural mapping of the surface of Falljökull has revealed that the moulins form steeply inclined pipe-like features which extend downward following the intersection between prominent down-ice dipping faults and several closely spaced ice-flow parallel fractures (Figures 6b, 6c, 6d, and 6e). Consequently, an alternative, structurally controlled mechanism for moulin development is proposed where these features are formed along fault planes during

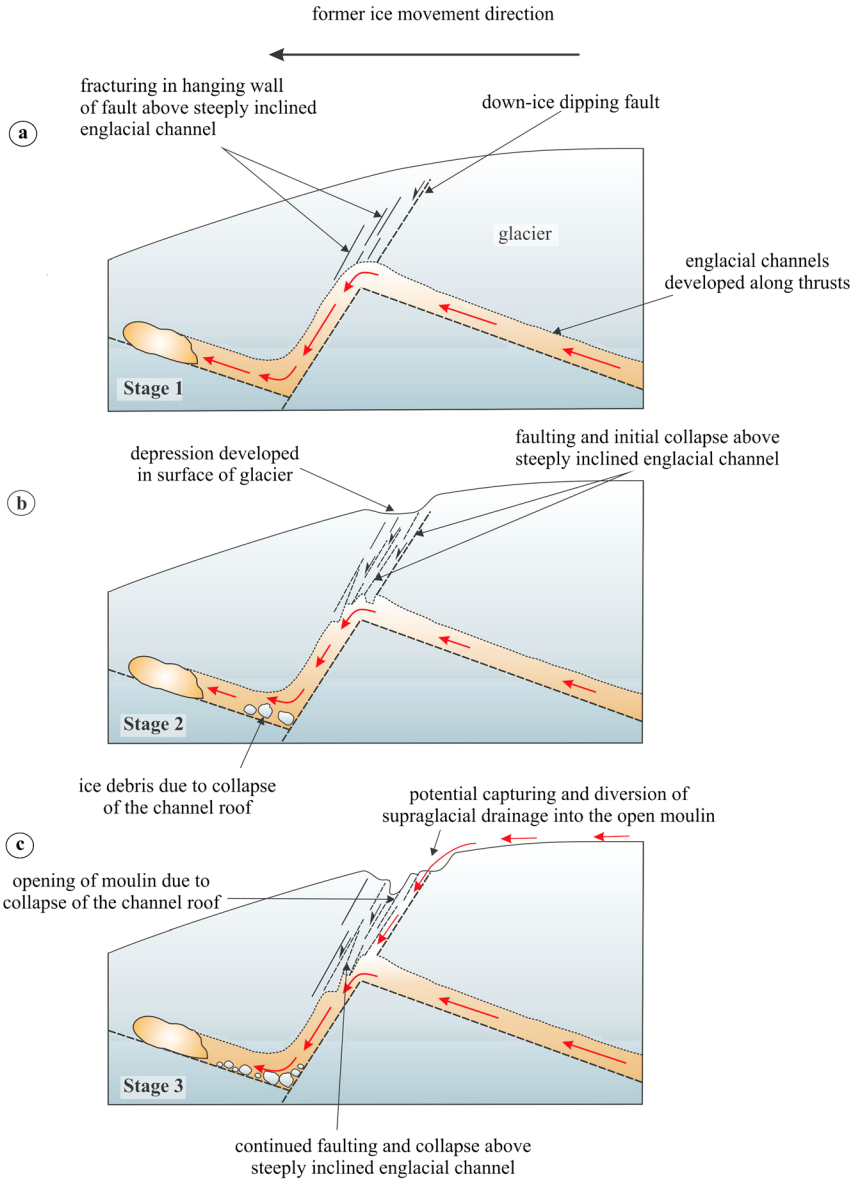

Figure 14. Three stage model of moulin formation relating it to the collapse of a steeply inclined englacial meltwater conduit formed along a down-ice dipping fault zone (see text for details).

rotational faulting and collapse at the margin of Falljökull (Figure 14). This three-stage model is illustrated in Figure 14 and links moulin formation to collapse of englacial drainage channels flowing along (strike-parallel) or down (down-dip) the main down-ice dipping faults, facilitated by the highly fractured nature of the ice within these fault zones (see Figures 1d, 5, 6b). The brittle faults controlling the multiple rotational slope failure of the margin of the glacier are extensional (normal) faults (Figure 13). Extension occurring across these faults would help in the formation of open cavities, such as englacial drainage channels and/or moulin, within the fault zones.

[49] The early stages of moulin formation (Stages 1 and 2, Figures 14a and 14b, respectively) result from the collapse of the highly fractured ice within fault zone into the englacial channels. During the winter, these channels are likely to empty as the glacial hydrogeological system closes down, effectively leaving the channel roof unsupported and more prone to collapse. Open englacial channels within the fault zone, as shown in Figure 14, could accommodate the blocks of ice falling from the roof, with meltwater flowing through the channel during the spring-summer helping to maintain this void space by removing the fallen ice, thereby facilitating continued moulin development. This process would eventually lead to the lowering of the glacier surface immediately above the developing moulin (Stage 2; Figure 14b); analogous to surface subsidence above mine workings. At Falljökull, surface subsidence associated with moulin development is thought to be responsible for the c. 50 m diameter shallow, highly fractured depression which encloses the three smaller moulin shown in Figure 6b. The rate and scale of the collapse, and the dimensions of the developing moulin, will be governed by the size of the englacial channel and the degree of fracturing within the fault zone.

[50] As the moulin continues to develop the open conduit marking this feature propagates toward the glacier surface following the fault zone (Stage 3, Figure 14c). This process will be aided by continued extensional movement across

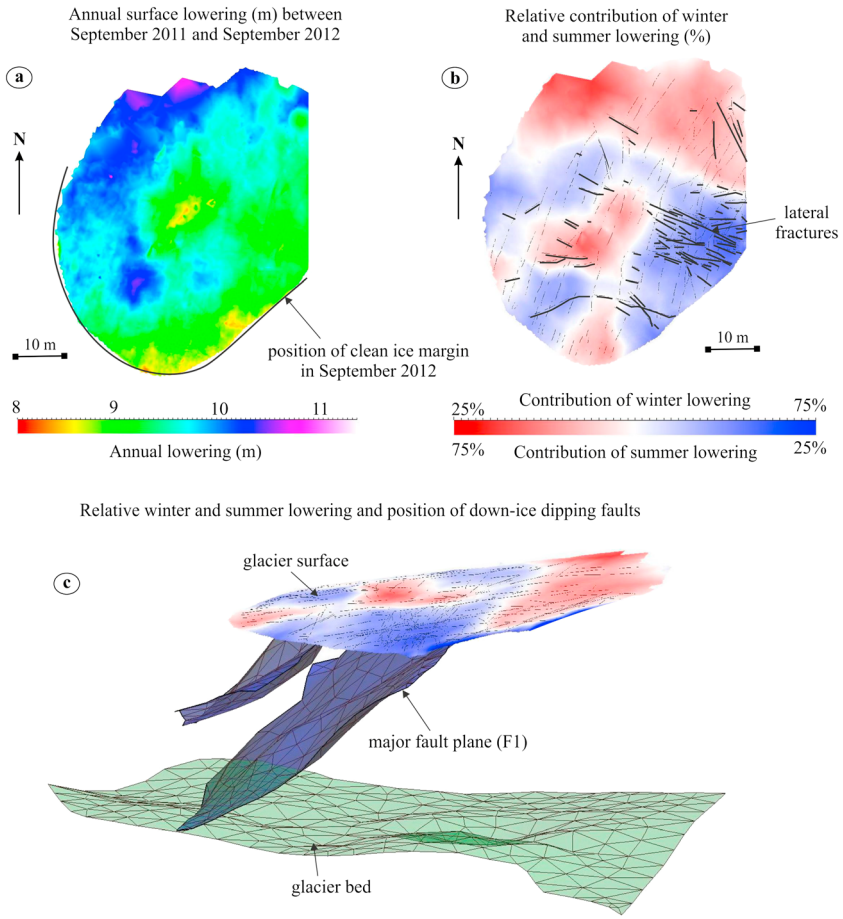

Figure 15. (a) Surface lowering of the Falljökull margin, between September 2011 and September 2012; (b) Relative contribution of winter and summer lowering to annual lowering at the Falljökull margin. Note the association of lateral fractures with the areas of greatest winter-dominated lowering; (c) Perspective view showing the position of major down-ice dipping faults in relation to winter-dominated surface lowering.

the fault, as well as erosion of the channel roof during periods of high meltwater discharge through the englacial system. Eventually, the moulin will breach the glacier surface (Stage 3, Figure 14c) with collapse of the fractured ice around the opening of the conduit leading to the formation of the cone-like depression marking the larger moulin on the surface of Falljökull (Figure 6d). A combination of surface subsidence and collapse around the open moulin may lead to the capture of any adjacent supraglacial drainage (Figure 14c) with meltwater flowing into the moulin from the surface of the glacier helping to maintain and enlarge this feature. The capturing of surface meltwater by the moulin will result in the linking of supraglacial and englacial drainage systems, as described in the literature [e.g., *Benn and Evans*, 2010]. Importantly, the development of the moulins and englacial drainage channels along the down ice dipping normal faults will further weaken the ice along these brittle deformation structures, therefore promoting or even accelerating collapse of the margin of Falljökull.

6.3. Structural Control on Changes in Glacier Surface Morphology

[51] The surface lowering of the clean ice margin of Falljökull over a 1 year period, based on the September 2011 and September 2012 lidar scans, is shown in Figure 15a. A lidar scan had not been included as part of the April 2012 field investigation. However, our observations of clear vertical offsets in the faults and distinct, stepped depressions on the glacier surface made it desirable to obtain a "rough" surface model for April 2012. This was achieved using the ~630 GPS positions associated with the April GPR surveys, and an additional 55 regularly spaced GPS measurements of ice surface, all collected using the Novatel Smart-V1 GPS antenna, which has given elevations within 1.5 m of the lidar data elsewhere in the Virkisjökull-Falljökull catchment. These measurements were interpolated using GOCAD™'s structural modeling workflow to derive an April 2012 surface.

[52] The April surface model allows the relative contributions of both winter lowering (September 2011–April 2012) and summer lowering (April 2012–September 2012) to annual surface lowering at the margin to be gauged (Figure 15b). There are clear zones of the glacier margin where winter lowering is dominant, accounting for 70% of the annual surface change. These zones are associated with the lateral surface faults that link with the main down-ice dipping fault planes (Figures 15b and 15c). These data suggest that near the margins of rapidly retreating temperate glaciers winter collapse, directed along the fault planes, could form a significant component of annual surface lowering that is not related to surface ablation. An implication of this is that structurally controlled collapse could cause differences

between mass balance calculations using direct measurements and geodetic methods near glacier margins. Ablation stakes were installed on the fractured zone of Falljökull in September 2012 to further test the structurally dominated and ablation-dominated components of annual lowering.

7. Conclusions

[53] The majority of Iceland's glaciers have been in retreat since at least the mid-1990s, with the rate of retreat having accelerated over the last decade. Since 2007, Falljökull in southeast Iceland has been undergoing passive downwasting and collapse, providing an ideal natural laboratory in which to study the range of deformation structures developed in response to ice-marginal retreat. The results of an integrated terrestrial LiDAR, Ground Penetrating Radar (GPR), and glaciological structural study have allowed the development of a detailed model of the surface and subsurface 3D structure of the margin of Falljökull. Collapse of the glacier margin takes the form of a multiple rotational failure where fault-bound blocks of ice rotate as they are displaced downslope. The large-scale, down-ice dipping normal faults which control this collapse are marked by zones of relatively intense brittle faulting (normal and reverse) and fracturing. The failure of the ice margin is pinned by a large area of buried ice which underlies the proglacial outwash deposited during the retreat of Falljökull. Pinning of the toe of the failure led to compression within fault block adjacent to the glacier margin and the formation of down-faulted graben-like structures within this block.

[54] Moulins developed within the marginal zone of Falljökull show a marked spatial relationship to the prominent normal faults controlling ice-margin collapse. This has led to an alternative model for moulin development where these features form in response to collapse of englacial drainage channels developed along faults within the ice. Once formed, the moulins may capture any surface meltwater channels resulting in the linking of supraglacial and englacial drainage systems. Importantly, the development of moulins and englacial drainage channels along the normal faults will further weaken the ice and therefore may promote or even accelerate collapse of the ice margin.

[55] Surface change models generated from the repeated surface lidar scans and GPS survey have shown that the mean seasonal ice surface loss in the period September 2011 to September 2012 was apparently greater during the winter when surface ablation would have been much lower. The complex pattern of surface loss within the marginal zone at Falljökull formed during the winter can be directly correlated to the main faults controlling the collapse of the ice margin. This evidence suggests that structurally controlled collapse may, in some instances, have a profound effect on glacier surface loss/mass balance calculations.

[56] **Acknowledgments.** This work forms part of ERP's IMP research project and the BGS-NERC Iceland Glacier Observatory project (http://www.bgs.ac.uk/research/glacierMonitoring/home.html?src=sfb). Jez Everest and Tom Bradwell are thanked for their comments on an earlier draft of the manuscript. Jez Everest, Tom Shanahan, Heiko Buxel, Alan MacDonald, Andrew Black, and Tom Bradwell are all thanked for their company, assistance, and good humor while in the field, as well as for the many discussions around the dinner table and over a beer (or two) at the end of a day on the ice. The reviewers Anders Schomacker, Jasper Knight, and John Menzies, and editors Bryn Hubbard and Poul Christoffersen are thanked for their constructive reviews and positive comments on an earlier version of this paper. This paper is published with the permission of the Executive Director of the British Geological Survey (NERC).

References

Allen, C. R., W. B. Kamb, M. F. Meier, and R. P. Sharp (1960), Structure of the Lower Blue Glacier, Washington, *J. Geol.*, *68*, 601–625.

Appleby, J. R., M. S. Brook, S. S. Vale, and A. M. MacDonald-Creevey (2010), Structural glaciology of a temperate maritime glacier: Lower Fox Glacier, New Zealand, *Geogr. Ann. Phys. Geogr.*, *92*, 451–467.

Arcone, S. A., D. E. Lawson, and A. J. Delaney (1995), Shortpulse radar wavelet recovery and resolution of dielectric contrasts within englacial and basal ice of Matanuska Glacier, Alaska, U.S.A., *J. Glaciol.*, *41*, 68–86.

Benn, D. I., and D. J. A. Evans (2010), *Glaciers and Glaciation*, Arnold, London, pp. 802.

Bennett, M. R., D. Huddart, and R. I. Waller (2000), Glaciofluvial crevasse and conduit fills as indicators of supraglacial dewatering during a surge, Skeiðarárjökull, Iceland, *J. Glaciol.*, *46*, 25–34.

Bradwell, T., O. Sigurdsson, and J. Everest (2013), Recent, very rapid retreat at a temperate maritime glacier in SE Iceland, *Boreas*., doi:10.1111/bor.12014. ISSN 0300–9483.

Danish Geodetisk Staff (1904), Öræfajökull, Sheet 87. Topographic map 1:50,000 scale. Geodetic Institute, Copenhagen.

Glasser, N. F., and T. A. Scambos (2008), A structural glaciological analysis of the 2002 Larsen B ice-shelf collapse, *J. Glaciol.*, *54*, 3–16.

Glasser, N. J., M. J. Hambrey, J. L. Etienne, P. Jansson, and R. Pettersson (2003), The origin and significance of debris-charged ridges at the surface of Storglaciären, northern Sweden, *Geogr. Ann. Phys. Geogr.*, *85A*, 127–147.

Goodsell, B., M. J. Hambrey, N. F. Glasser, P. Nienow, and D. Mair (2005), The structural glaciology of a temperate valley glacier: Haut Glacier d'Arolla, Valais Switzerland, *Arctic Antarct. Alpine Res.*, *37*, 218–232.

Guðmundsson, H. J. (1997), A review of the Holocene environmental history of Iceland, *Quaternary Sci. Rev.*, *16*, 81–92.

Gusmeroli, A., P. Jansson, R. Pettersson, and T. Murray (2012), Twenty years of cold surface layer thinning at Storglaciären, sub-Arctic Sweden, 1989–2009, *J. Glaciol.*, *58*, 3–10.

Hambrey, M. J., and A. G. Milnes (1977), Structural geology of an Alpine glacier (Griesgletcher, Valais, Switzerland), *Eclogae Geol. Helv.*, *70*, 667–684.

Hambrey M. J., T. Murray, N. F. Glasser, A. Hubbard, B. Hubbard, G. W. Stuart, and S. Hansen (2005), Structure and changing dynamics of a polythermal valley glacier on a centennial time-scale: midre Lovénbreen, Svalbard, *J. Geophys. Res.*, *110*, F01006, doi:10.1029/2004JF000128.

Herbst, P., F. Neubauer, and M. P. J. Schopfer (2006), The development of brittle structures in an alpine valley glacier: Pasterzenkees, Austria, 1887–1997, *J. Glaciol.*, *52*, 128–136.

Huddleston, P. J., and R. L. Hooke (1980), Cumulative deformation in the Barnes Ice Cap and implications for the development of foliation, *Tectonophysics*, *66*, 127–146.

Jóhannesson, T., and O. Sigurðsson (1998), Interpretation of glacier variations in Iceland 1930–1995, *Jökull*, *45*, 27–33.

Lawson, W. (1996), Structural evolution of variegated Glacier, Alaska, USA, since 1948, *J. Glaciol.*, *42*, 261–270.

Lawson, W., M. J. Sharp, and M. J. Hambrey (1994), The structural glaciology of a surge-type glacier, *J. Struct. Geol.*, *16*, 1447–1462.

Mallet, J. L. (1997), Discrete modeling for natural objects, *Math. Geol.*, *29*, 199–219.

Murray, T., and A. D. Booth (2010), Imaging glacial sediment inclusions in 3-D using ground-penetrating radar at Kongsvegen, Svalbard, *J. Quaternary Sci.*, *25*, 754–761.

Murray, T., G. W. Stuart, M. Fry, N. H. Gamble, and M. D. Crabtree (2000), Englacial water distribution in a temperate glacier from surface and borehole radar velocity analysis, *J. Glaciol.*, *46*, 389–398.

Navarro, F. J., Y. Y. Macheret, and B. Benjumea (2005), Application of radar and seismic methods for the investigation of temperate glaciers, *J. Appl. Geophys.*, *57*, 193–211.

Sensors and Software (2003), *Pulse EKKO PRO user's guide*, Sensors and Software Inc., Mississauga, Canada, pp. 159.

Sharp, M. (1988), Surging glaciers – behaviour and mechanisms, *Progr. Phys. Geogr.*, *12*, 349–370.

Sharp, M., W. Lawson, and W. Anderson (1988), Tectonic processes in a surge type glacier, *J. Glaciol.*, *40*, 327–340.

Sigurðsson, O., T. Jónsson, and T. Jóhannesson (2007), Relation between glacier-termini variations and summer temperatures in Iceland since 1930, *Ann. Glaciol.*, *42*, 395–401.

Waltham, T. (2010), *Foundations of Engineering Geology*, 3rd ed., Spon Press, London and New York.

Woodward, J., and M. J. Burke (2007), Applications of ground-penetrating radar to glacial and frozen materials, *J. Environ. Eng. Geophys.*, *12*, 69–85.

Woodward, J., T. Murray, and A. McCraig (2002), Formation and reorientation of structure in surge-type glacier Kongsvegen, Svalbard, *J. Quaternary Sci.*, *17*, 201–209.